Cite as: Esteban-Manzanares, G., González-Bermúdez, B., Cruces, J. et al. Improved Measurement of Elastic Properties of Cells by Micropipette Aspiration and Its Application to Lymphocytes. Ann Biomed Eng 45, 1375–1385 (2017). https://doi.org/10.1007/s10439-017-1795-7.

Improved Measurement of Elastic Properties of Cells by Micropipette Aspiration and Its Application to Lymphocytes

Gustavo Esteban-Manzanares[1,2], Blanca González-Bermúdez[1,2], Julia Cruces[3], Mónica De la Fuente[3], Qingxuan Li[1,2], Gustavo V. Guinea[1,2], José Pérez-Rigueiro[1,2], Manuel Elices[1,2], Gustavo R. Plaza[1,2]

[1] Center for Biomedical Technology. Universidad Politécnica de Madrid, 28223 Pozuelo de Alarcón, Spain.

[2] Departamento de Ciencia de Materiales, ETSI de Caminos, Canales y Puertos. Universidad Politécnica de Madrid, 28040 Madrid, Spain.

[3] Departamento de Fisiología Animal II, Facultad de Biología, Universidad Complutense de Madrid, E-28040, Madrid, Spain.

ABSTRACT

Mechanical deformability of cells is an important property for their function and development, as well as a useful marker of cell state. We provide here a method to measure the two basic mechanical parameters, elastic modulus and Poisson's ratio, of the cellular material under the approximation of homogeneous isotropic linear elasticity. The proposed method is based on the analysis of micropipette aspiration experiments. We applied this procedure to measure the elastic parameters of lymphocytes, in which the mechanical properties depend on their activation state. The proposed method to assess elastic parameters may be implemented in future technologies for the automated measurement of mechanical properties of cells, based on the micropipette aspiration technique. These measurements would be useful in clinical practice.

Keywords

Cell deformability, mechanical properties of cells, micropipette aspiration, elastic parameters

Cite as: Esteban-Manzanares, G., González-Bermúdez, B., Cruces, J. et al. Improved Measurement of Elastic Properties of Cells by Micropipette Aspiration and Its Application to Lymphocytes. Ann Biomed Eng 45, 1375–1385 (2017). https://doi.org/10.1007/s10439-017-1795-7.

INTRODUCTION

Several studies have established that the mechanical properties of cells are useful markers of cell state (1). Furthermore, the deformability of cells is a promising biomarker for various disease processes and changes in cell state, and is based on the associated cytoskeletal and nuclear changes (2-4).

Mechanical deformability is particularly important in cell migration, which plays a vital role especially in blood and immune cells, since their activity is dependent on the ability to flow through narrow channels. In the case of phagocytic cells (neutrophils and monocytes), previous works studied their deformability showing how this property may change upon stimulation with chemokines associated with infection or stress (5-7). In addition, stiffening of red blood cells by malaria parasite can block locally the blood flow, while the migration of cancer cells is facilitated by their higher deformability (8). Also deformability of stem cells plays a major role in their ability to migrate, which is crucial for tissue regeneration (9, 10). As an example, we showed in a previous study that a higher deformability of mesenchymal stem cells (cardiac mesoangioblasts) was related to an improved behavior in tissue regeneration (11). Additionally mechanical cues are determinant for the fate of stem cells (12, 13). This importance of the mechanical properties justifies the interest in developing simple procedures to measure these properties of cells in an automatic or nearly-automatic manner. Some of the procedures currently under development are based on the micropipette aspiration technique, and we propose here a methodology to compute the two basic elastic parameters, i.e. elastic modulus and Poisson's ratio, in the frame of a first-order description of the cell as a homogeneous linear elastic material.

The available techniques (14, 15) for the mechanical characterization of cells use different methods to apply a mechanical deformation and measure the corresponding force. (i) The micropipette-aspiration technique consists of aspirating the cell by a microcapillary and analyzing the aspirated length corresponding to a given suction pressure (16). This allows the computation of elastic or viscoelastic parameters for low deformations under the assumption of incompressibility (17) or the cytoplasm apparent viscosity for large deformation (18). In this work we propose to measure a second variable, which allows measuring two elastic parameters, as explained below. Among the various techniques to measure the mechanical properties of cells, micropipette aspiration is one of less demanding to implement in a laboratory, due to the simplicity of the experimental device and the way the tests are carried out, although the analysis of the measurements is more complicated and requires digital image processing. Micropipette aspiration is usually applied to nonadherent cells, with largely spherical symmetry (19), and can be applied also to suspended adherent cells (18). (ii) Atomic force microscopy is based on the deflection of a cantilever with a tip which is indented into a specific location of a cell, and usually is applied to measurements on adherent cells (20), though it can be used for non-adherent cells when fixed on a substrate (21). (iii) In magnetic twisting rheology (22), the response of a cell-attached magnetic bead is probed in response to an external magnetic field. Indentation by atomic force microscopy or magnetic-beads twisting probe the deformation of a small region of the

cell and therefore allow measuring the local properties. In a different way, micropipette aspiration applies large deformations to the whole cell and measures its global response.

Various promising approaches are being developed with the aim of performing measurements of mechanical properties of very large numbers of cells. (iv) The optical stretching technique uses optical-gradient forces to stretch the cell (23). An important limitation of this technique is the heating of the cells. (v) Deformability cytometry is a hydrodynamic approach, in which cells are deformed by deceleration at the stagnation point of fast extensional flow (2). (vi) Another group of automatic-measurement techniques consists of measuring the transit time as cells pass through flow constrictions, single or multiple pores (24). (vii) The automatic measurement of properties based on the micropipette aspiration technique is closely related to the previous group of techniques.

At low deformations, the cell behaves like a solid (25, 26) and analyzing its mechanical properties allows the identification of the role played by the different internal components (25, 27, 28), complementing other studies, in particular of the cytoskeleton (29). Several mechanical models have been developed, including those appropriate to measure the shear stiffness of the red-blood-cell membrane (30), the cortical tension for a cell considered a spherical drop of negligibly-viscous fluid with a contractile cortex (19) or the apparent viscosity of the cell during its large-deformation flow into the micropipette (18, 31, 32). Other biophysical models were developed for particular cells in which the cytoskeletal components may dictate the behavior during the micropipette aspiration process (27, 33, 34).

Previous works have provided methods to assess, from micropipette-aspiration experiments, the elastic modulus (17, 35-37). However, all those works assumed incompressibility, i.e. Poisson's ratio of 0.5. In this context, our aim was to develop a methodology to measure both the elastic modulus and the Poisson's ratio by using micropipette aspiration taking into account the intrinsic geometric nonlinearity of the problem. We explain here the proposed two-step procedure to assess the elastic parameters. In the following sections, we analyze and discuss the mechanical model, and we compare our results and the equations developed in previous studies. Using this simple procedure, we estimated the elastic parameters of one relevant kind of cell, the lymphocyte, in which the application of this enhanced methodology was evaluated. These cells depend on their deformability to reach the focus of infections and recognize the antigens, allowing an appropriate immune response (38). Moreover, the adequate functioning of these cells is related to the health state of the organism (39).

We consider that the methodology used in this study will facilitate the carrying out of large-scale studies of the relation between physicochemical cues or diseases and the mechanical behavior of cells. Systematic studies of the deformability of lymphocytes could provide new insights in studies of immunosenescence, biocompatibility and infection. Characterizing the mechanical properties of these cells will be of interest for clinical and pre-clinical applications, especially in the field of infection processes and immunosenescence.

MATERIALS AND METHODS

Finite elements model

The commercial finite element software Abaqus (Dassault Systèmes Simulia Corp., Tustin, USA) has been used to perform the finite element analysis. We have built an axisymmetric model (see figure 1) of a spherical cell, using the Abaqus preprocessor. The mesh of the spherical cell contains four- and three-nodes elements (CAX4H, CAX3H), with first-orden interpolation and hybrid formulation. The mesh is finer on the zone close to the contact with the rigid surface of the microcapillary. The cell material is assumed to be linear-elastic. The surface of the microcapillary is modeled as a rigid surface and contains a filet radius R_f (see figure 1 and discussion about its value in the text). In the model, lengths and displacements are measured in units of the internal radius of the micropipette, R_p, and pressure and stresses in units of the elastic modulus E.

The contact between the spherical cell and the surface of the microcapillary is assumed frictionless. The radial displacement is impeded for the nodes on the axis of symmetry. The differential (suction) pressure ΔP is applied on the surface of the cell placed inside the micropipette (at the bottom of figure 1b) (36).

Convergence of the calculations was achieved by progressively doubling the number of nodes on the boundaries until differences in iterated displacements were under 0.4%.

Cells

We used female ICR-CD1, *Mus musculus*, mice (Janvier S.A.S., Le Genest-St-Isle, France). Animals were treated according to the guidelines of the European Community Council Directives 1201/2005 EEC and the experimental protocol was approved by the Animal Ethics Committee of the Universidad Complutense de Madrid (Spain). Peritoneal leukocytes were obtained from mice, by injecting intraperitoneally 3 ml of sterile Hank's solution, previously tempered at 37ºC. After massaging the abdomen, 80 % of the injected volume was recovered. Non-adherent lymphocytes were isolated by incubating the peritoneal leukocyte population at 37 ºC in a humidified atmosphere of 5% CO_2, for 45 minutes, using migratory inhibitory factor (MIF) plates (Kartell, Noviglio, Italy). The supernatants were collected using a Pasteur pipette. Starting lymphocyte concentration was of the order of 10^5 cell/ml. Cells were maintained at 4ºC until the micropipette aspiration experiments.

Micropipette aspiration experiments

Micropipette aspiration experiments were conducted in a custom-built device (11, 18) similar to those described previously (40), using microcapillaries with a nominal internal diameter of 5 µm. The suspension of cells (~0.25 mL) was deposited on a cover-glass plate placed in an optical Meiji TC5400 inverted microscope. The microcapillary was connected to a distilled water reservoir and the differential pressure was applied by a difference in height of the reservoir with respect to the cells dispersion. The differential pressure ΔP was increased at a rate of 0.5 Pa/s, as sketched in Figure 6c. The aspiration process was recorded by time-lapse imaging.

Automatic digital analysis

Recorded images were analyzed to measure the internal radius of the micropipette R_p, the initial radius of the cell R_c, the aspirated length L_p and the reduction of the transversal diameter ΔD_t (see figure 1). We used MATLAB (Mathworks, Natick, Massachusetts) to automatically analyze the sequence of images acquired in each experiment. A specific script with automatic thresholding and segmentation was developed to identify the area around the tip of the microcapillary, the microcapillary wall and the boundary of the cell and to compute the mechanical parameters.

MODEL

The cell is described as a homogeneous, isotropic linear-elastic sphere. As shown in Figure 1b, during the aspiration process there is a radial displacement of the cell material, and it is possible to compute the transversal contraction of the cell, ΔD_t (see Figure 1), due to the aspiration process. Use of the two variables, L_p and ΔD_t, allows estimating the two parameters of the linear elastic material, the elastic modulus E and the Poisson's ratio ν, as explained below.

Even for a linear elastic material, the aspiration of an elastic sphere constitutes a case of structural non-linearity due to the contact (41) and also to the slipping between the deformable sphere and the rigid surface of the micropipette. Consequently, the relationship between the differential suction pressure ΔP (pressure in the medium in which the cell is suspended minus pressure inside the microcapillary) and the aspirated length is nonlinear, as demonstrated by the results below.

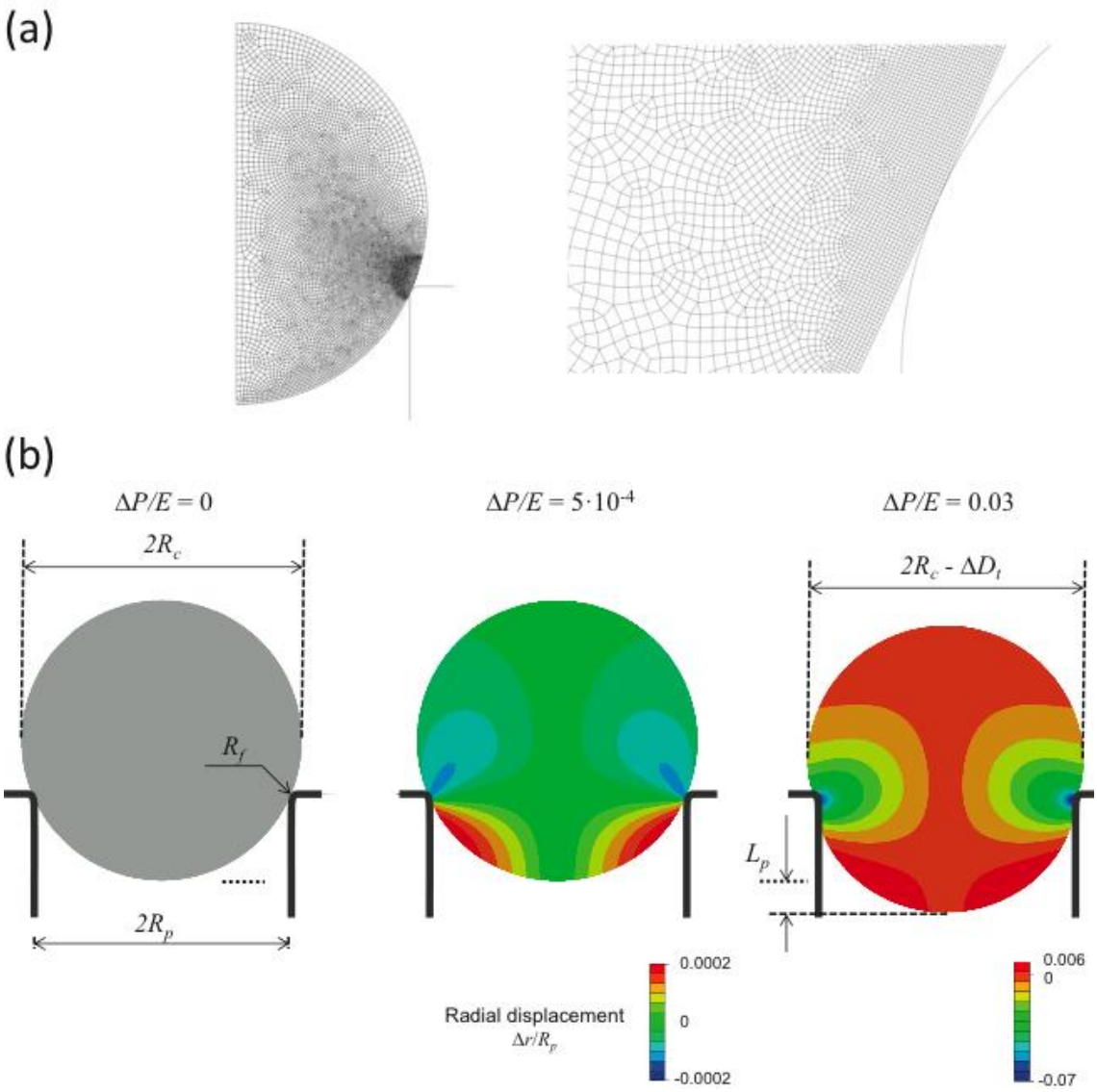

Figure 1. Numerical model. (a) Mesh used in the computations, with smaller elements in the region of the contact with the micropipette. (b) Scheme showing the geometrical parameters and an example of the distribution of radial displacements for R_c/R_p = 1.1, R_f/R_p = 0.05, ν = 0.3. R_p, internal radius of the pipette; R_c, initial radius of the cell; ΔD_t, reduction of the maximum transversal-section diameter; L_p aspirated length.

COMPUTED ASPIRATION CURVES

Effect of fillet radius

The geometric parameters for the analysis are the nondimensional radius of the cell R_c/R_p and the fillet radius R_f/R_p. The third parameter is the Poisson's ratio ν. The transversal contraction $\Delta D_t/R_p$, the aspirated length L_p/R_p and the nondimensional aspiration pressure $\Delta P/E$ are the variables analyzed for each set of parameters. In the aspiration experiments, the relative radius of the cell R_c/R_p is measured optically but the filet radius cannot be measured optically because of its small size (see for instance Figure 6a below). This cloud be the reason why the fillet radius is not considered in previous works (35-37).

Figures 2a and 2c show, respectively, the curves for the nondimensional pressure $\Delta P/E$ and transversal contraction $\Delta D_t/R_p$, versus the nondimensional aspirated length L_p/R_p, for five values of the Poisson's ratio ν and three values of the nondimensional fillet radius R_f/R_p. In the figure, the radius of the cell is kept constant R_c/R_p=1.15. Apart from the effect of the cell radius, the figure shows that both the Poisson's ratio and the fillet radius have an important influence on the curves. Therefore, a priori the fillet radius cannot be neglected when computing the elastic parameters of the aspirated cell.

The value of the fillet radius measures the sharpness of the contact between the cell and the microcapillary. Additionally, the contact area will also depend on the roughness of the cell. Consequently a very small value for the fillet radius (measured, for instance, by electron microscopy) would not be realistic for modeling the contact since the physical contact area would be larger due to the ruffles and microvilli of the cell. Therefore, the value of the fillet radius used in the model is more a contact parameter that must be in agreement with the roughness of the cell. As shown in the next lines, it is possible to estimate reasonably a practical value $R_f = R_p/20$, which has been used in the calculations here. On one side, for the micropipettes typically used in aspiration experiments, with internal radius R_p between 5 and 10 μm, the fillet radius R_f is very tiny and clearly smaller than the resolution in an optical microscope (Figure 6a). On the other side, the value of R_f used in the model must be at least of the order of magnitude of the roughness of the cell surface, due to the ruffles and microvilli. For the small blood cells typically tested with 5-μm micropipettes, the cell-surface roughness is of the order of 0.1 μm (42), and for larger suspended cells that can be aspirated with a micropipette of $R_p \sim 10$ μm the roughness is approximately twice larger (43). This reasoning justifies using $R_f \sim R_p/20$.

Following the previous reasoning, we propose in this work to compute the elastic parameters of the cell by assuming $R_f/R_p = 0.05$. The elastic modulus and Poisson's ratio are labelled, for this reason, $E_{0.05}$ and $\nu_{0.05}$.

Cite as: Esteban-Manzanares, G., González-Bermúdez, B., Cruces, J. et al. Improved Measurement of Elastic Properties of Cells by Micropipette Aspiration and Its Application to Lymphocytes. Ann Biomed Eng 45, 1375–1385 (2017). https://doi.org/10.1007/s10439-017-1795-7.

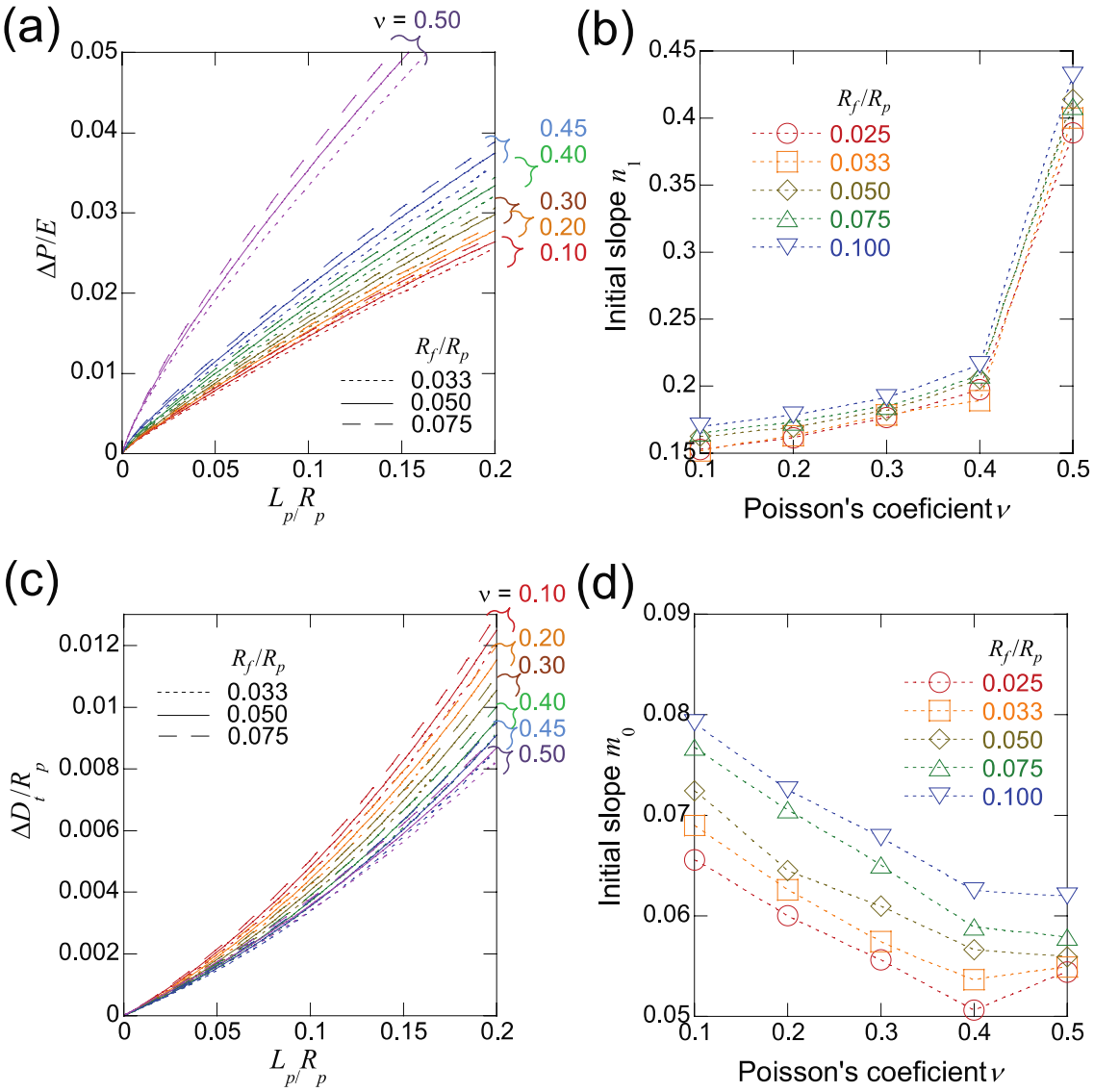

Figure 2. Aspiration curves for various values of the fillet radius and Poisson's ratio, for cell size R_c/R_p = 1.5. (a) Nondimensionalized pressure vs. aspirated length; (b) initial slope of the pressure-length curves vs. Poisson's ratio; (c) transversal contraction-aspirated length ratio vs. nondimensionalized aspirated length; (d) initial slope of the transversal contraction-length curves vs. Poisson's ratio. The initial slopes in (b) and (d) were obtained by fitting the corresponding curves in (a) and (c) to equations 4 and 1 in the range $0 < L_p/R_p < 0.3$.

Comparison with previous works

The three previous works mentioned above analyzed the aspiration process considering a cell of homogeneous isotropic elastic material. In two the three works, the cell was assumed incompressible, i.e. with a Poisson's ratio $\nu = 0.5$ in the linear elastic regime. Theret et al. modeled the cell as a linear-elastic incompressible half-space (35). In their analytic solution, the nonlinearities due to the contact of the two solids and the sliding between them were not taken into account. Zhou et al. considered an incompressible neo-Hookean material and took into account the nonlinearities (36). By fitting their numerical results, they obtained an equation relating pressure, aspirated length, geometrical constants and elastic modulus. Li and Chen analyzed the problem modeling the cell as a linear elastic material (37). In their numerical study, the effect of the nonlinearities was not analyzed. They also proposed an equation obtained by fitting the numerical results. The equations developed in those three works can be used to estimate the elastic modulus of the cell from the experimental curves differential pressure vs. aspirated lengths.

In the linear-elastic incompressible half-space model by Theret et al. (35) the nondimensional differential pressure $\Delta P/E$ is proportional to the nondimensional aspirated length L_p/R_p and independent of the cell size. In the other two works, this ratio – obtained by numerical fitting – depends on the cell radius.

One important limitation to fit the curves differential pressure vs. aspirated length is the nonlinearity of the problem, which may produce different results depending on the range of values for which the fitting is performed. To compare the previous models and our results (with $\nu = 0.5$ and $R_f/Rp = 0.05$), we have computed the initial slope (tangent at origin) of the curves $\Delta P/E$ vs. L_p/R_p for three different ranges of values: (i) for very small deformation ($0 < L_p/R_p < 0.001$), (ii) for a range of realistically measurable displacements in an aspiration experiment ($0 < L_p/R_p < 0.3$), and (iii) an intermediate range is also included. These values are shown in Figure 3.

Figure 3 shows firstly the inaccuracy of the equation developed by Theret et al. due to its limitations (infinite size of the cell and nonlinearities not included in the model). At very large values of R_c/R_p, the slope provided by that equation coincides with the initial slope in the range of very small deformations, $L_p/R_p < 0.001$. The figure also shows that the initial slope provided by Zhou et al.'s equation is similar (in its range of validity) to the initial slope estimated in this work for moderate displacements, L_p/R_p up to 0.1-0.3. Finally, Li and Chen's equation gives an initial slope similar to the initial slope in our curves ($L_p/R_p < 0.001$) for cell sizes relatively large, $R_c/R_p \geq 2.3$.

An equation that provides the initial slope ($L_p/R_p < 0.001$) of the curve $\Delta P/E$ vs. L_p/R_p is not of practical use because of the impossibility of measuring optically very small displacements of the front of the aspirated cell. The need to develop a procedure to estimate the elastic parameters in an aspiration experiment implies that a practical equation should fit the curve $\Delta P/E$ vs. L_p/R_p in a range of displacements that can be realistically measured and we propose the range $0 < L_p/R_p < 0.3$. In the next paragraphs we describe the proposed procedure.

Cite as: Esteban-Manzanares, G., González-Bermúdez, B., Cruces, J. et al. Improved Measurement of Elastic Properties of Cells by Micropipette Aspiration and Its Application to Lymphocytes. Ann Biomed Eng 45, 1375–1385 (2017). https://doi.org/10.1007/s10439-017-1795-7.

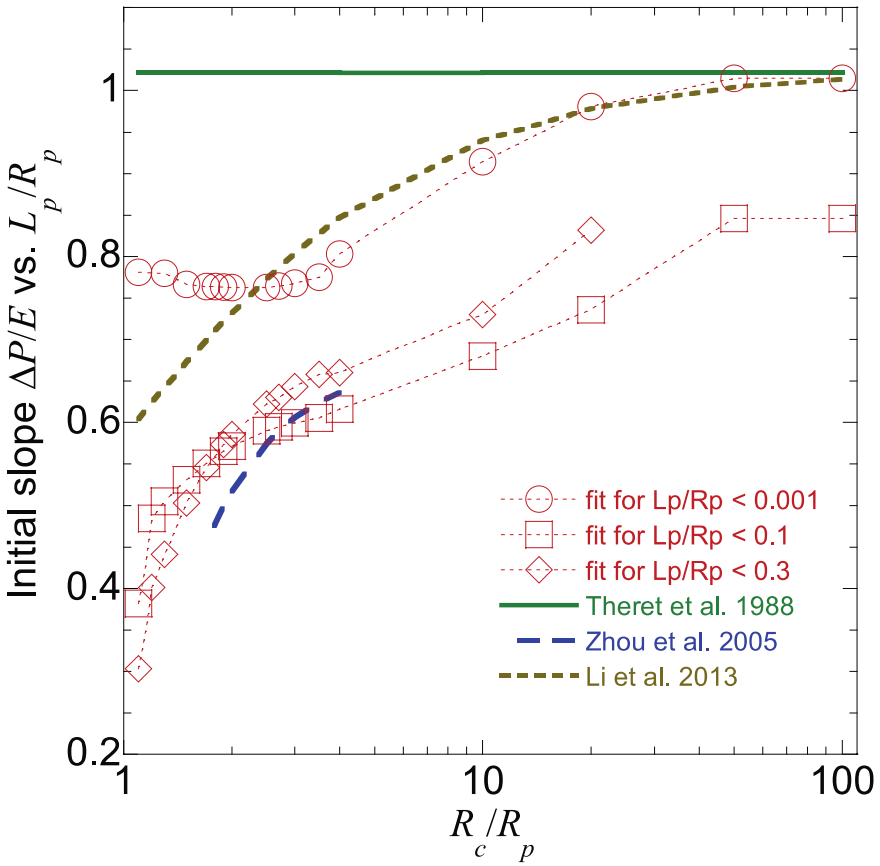

Figure 3. Initial slope of the curve $\Delta P/E$ vs. L_p/R_p in the equations developed by Theret et al. (35), Zhou et al. (17, 36), Li and Chen (37) and in the curves obtained in this work (with $\nu = 0.5$ and $R_f/Rp = 0.05$), obtained by fitting them to the equation 4, in the ranges $0 < L_p/R_p < 0.001$, $0 < L_p/R_p < 0.1$ and $0 < L_p/R_p < 0.3$. Zhou et al. developed their equation for the range $5/3 < R_c/R_p < 4$.

PROPOSED PROCEDURE TO ASSESS THE ELASTIC PARAMETERS

Procedure to evaluate the Poisson ratio

The relationship between the transversal contraction ΔD_t and the displacement of the cell front L_p, as a function of the Poisson's ratio ν, has been studied to obtain an expression to evaluate ν. As an example, Figure 4a shows $\Delta D_t/R_p$ versus L_p/R_p, for various values of ν and for a constant cell radius $R_c/R_p = 1.1$. We found that the curves can be conveniently fitted to the expression

$$\frac{\Delta D_t}{R_p} = m_1\left(1+\frac{L_p}{R_p}\right)^{m_2}\left(e^{m_3\frac{L_p}{R_p}}-1\right) \qquad (1)$$

The parameters m_1, m_2 and m_3 depend on the Poisson's ratio and the radii ratio R_c/R_p. The slope of the curve at the origin is $m_0 = m_1 m_3$. We computed the slope m_0 for each curve, using equation 1 to fit the curve in the range $0 < L_p/R_p < 0.3$. We studied the slope at the origin as a function of ν and R_c/R_p, as shown in figure 4b, obtaining by fitting the following expression (surface shown in figure 4b):

$$m_0 = \frac{1}{\alpha_1}\left[1+\alpha_2\frac{R_c}{R_p}+\alpha_3\left(\frac{R_c}{R_p}\right)^2\right]\left[1-\left(\frac{\nu_{0.05}}{\alpha_4}\right)^{\alpha_5}\right] \qquad (2)$$

where the numerical values of the constants are given in Table 1. Poisson's ratio can be deduced from equation (2):

$$\nu_{0.05} = \alpha_4\left\{1-\alpha_1 m_0\left[1+\alpha_2\frac{R_c}{R_p}+\alpha_3\left(\frac{R_c}{R_p}\right)^2\right]^{-1}\right\}^{1/\alpha_5} \qquad (3)$$

Practically, to compute ν one has to, first, fit equation (1) to the experimental results and obtain $m_0 = m_1 m_3$, and then use equation (3) with the corresponding cell size R_c/R_p . Note that with this procedure only experimental kinematic variables are used, not needing to take into account values of the differential pressure ΔP during the experiment.

Cite as: Esteban-Manzanares, G., González-Bermúdez, B., Cruces, J. et al. Improved Measurement of Elastic Properties of Cells by Micropipette Aspiration and Its Application to Lymphocytes. Ann Biomed Eng 45, 1375–1385 (2017). https://doi.org/10.1007/s10439-017-1795-7.

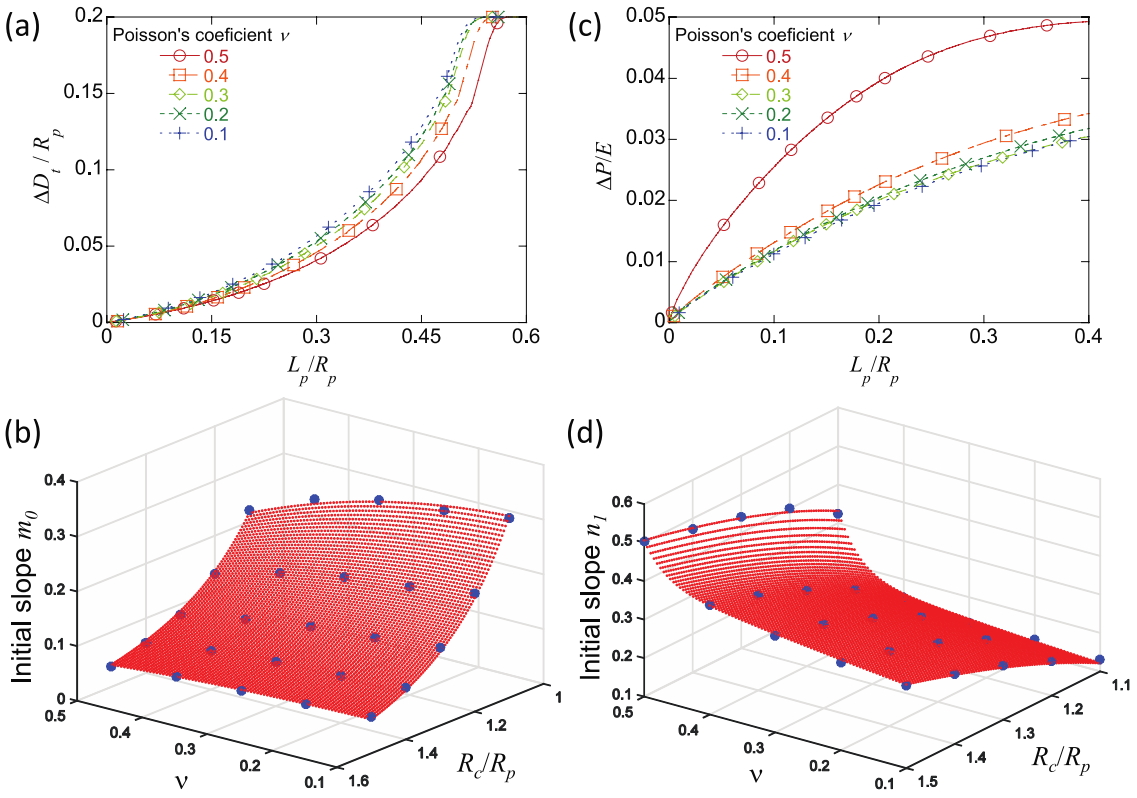

Figure 4. Fitting the numerical results to obtain the equations allowing computing the elastic parameters ν and *E*. (a) Nondimensionalized radial contraction vs. aspirated length for the case R_c/R_p = 1.1 and R_f/R_p = 0.05; (b) values of the initial slope of curves in (a) as a function of ν and R_c/R_p (dots) and surface obtained by fitting equation 2. (c) Nondimensionalized differential pressure vs. aspirated length for the case R_c/R_p = 1.1 and R_f/R_p = 0.05; (d) values of the initial slope of that type of curves as a function of ν and R_c/R_p (dots) and surface obtained by fitting equation 5.

Procedure to evaluate the elastic modulus

Evaluating the elastic modulus of the cell during the experiment requires taking into account the differential pressure ΔP. As an example, figure 4c shows the curves differential pressure vs. displacement of the cell front L_p, for different values of ν and for the ratio R_c/R_p = 1.1. Each curve was fitted, in the range $0 < L_p/R_p < 0.3$, to the expression

$$\frac{\Delta P}{E} = n_1\left(\frac{L_p}{R_p}\right) + n_2\left(\frac{L_p}{R_p}\right)^2 \qquad (4)$$

where the parameters n_1 and n_2 depend, again, on the Poisson's ratio and the radii ratio R_c/R_p. We studied this dependence for n_1, as shown in figure 4d, obtaining by fitting the following expression (surface shown in figure 4d):

$$n_1 = \frac{1+\beta_1 \nu_{0.05}{}^{\beta_2} + \beta_3 R_c/R_p}{1+\beta_4 R_c/R_p} \qquad (5)$$

where the numerical values of the constants are shown in Table 2.

The parameter n_1, that gives the initial slope of the $\Delta P/E$ *vs.* L_p/R_p curve, can be calculated from the Poisson's ratio, obtained previously, and the radii ratio R_c/R_p.

Once n_1 is known, the elastic modulus E can be estimated by:

$$\Delta P = En_1\left(\frac{L_p}{R_p}\right) + En_2\left(\frac{L_p}{R_p}\right)^2 \qquad (6)$$

where $En_1 = [d(\Delta P/E)/d(L_p/R_p)]_0$ is the experimental initial slope.

The previous equations have been obtained for the range $1.1 < R_c/R_p < 1.5$, because for large cell sizes the relative transversal contraction D_t/R_p is too small in the regime of moderately small deformations.

Figure 5 summarizes the procedure to estimate both the Poisson's ratio and the elastic modulus from the experimental data.

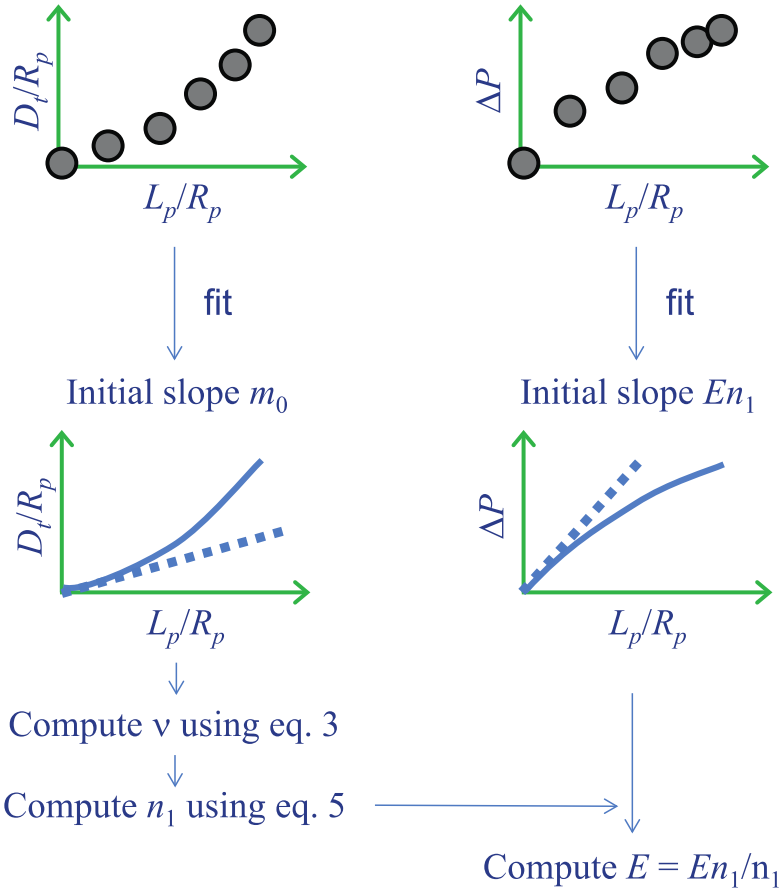

Figure 5. Scheme showing the proposed procedure to compute the elastic parameters ν and *E*.

MECHANICAL CHARACTERIZATION OF LYMPHOCYTES

We performed micropipette experiments of lymphocytes in order to study the possibilities of characterizing their mechanical behavior using the models published previously and, specially, the procedure developed in this work and described in the previous sections. As explained in the section of materials and methods, we were able to perform an automatic analysis of the image sequences acquired in during the aspiration experiments. In total we analyzed 312 lymphocytes. A ramp of differential pressure $d(\Delta P)/dt$ = 5 Pa/s was applied, as schematized in Figure 6c.

By applying the linearized expression of the Zhou et al.'s equation (17, 36), we estimated an elastic modulus $E_{\nu=0.5}$ = 536 ± 2 Pa (mean value ± standard error) for the first stage of the aspiration process ($L_p < 1.5R_p$).

In the experiments, the aspiration process continued until the cell was completely suctioned into the microcapillary (see the videos provided as supplementary material). When a cell undergoes large deformations, it evolves from a solid-like to a fluid-like state (25, 26). In fact, when the whole cell is completely aspirated by a micropipette, the liquid-like cellular material flows in the microcapillary and it is possible to quantify the apparent viscosity (19, 32). We, therefore, quantified the apparent viscosity of lymphocytes following the methodology described in our previous work (18), and obtained the value 295 ± 1 Pa·s.

We used the procedure described in Figure 5 to estimate the elastic modulus and Poisson's ratio of lymphocytes. The procedure requires cells with a radius close to the micropipette radius, so that equation 1 can be applied to fit the experiments. Among the whole set of experiments performed in this work we found five samples with a cell size close to $1.1R_p$. We measured computed $\Delta D_t/R_p$ and L_p/R_p at any time. As an example, figure 6d-e show the experimental values and the curves obtained by fitting the equations in the range $0 < L_p/R_p < 0.3$. For this reduced set of experiments, we obtained the values $\nu_{0.05}$ = 0.33 ± 0.11 and $E_{0.05}$ = 800 ± 300 Pa.

Cite as: Esteban-Manzanares, G., González-Bermúdez, B., Cruces, J. et al. Improved Measurement of Elastic Properties of Cells by Micropipette Aspiration and Its Application to Lymphocytes. Ann Biomed Eng 45, 1375–1385 (2017). https://doi.org/10.1007/s10439-017-1795-7.

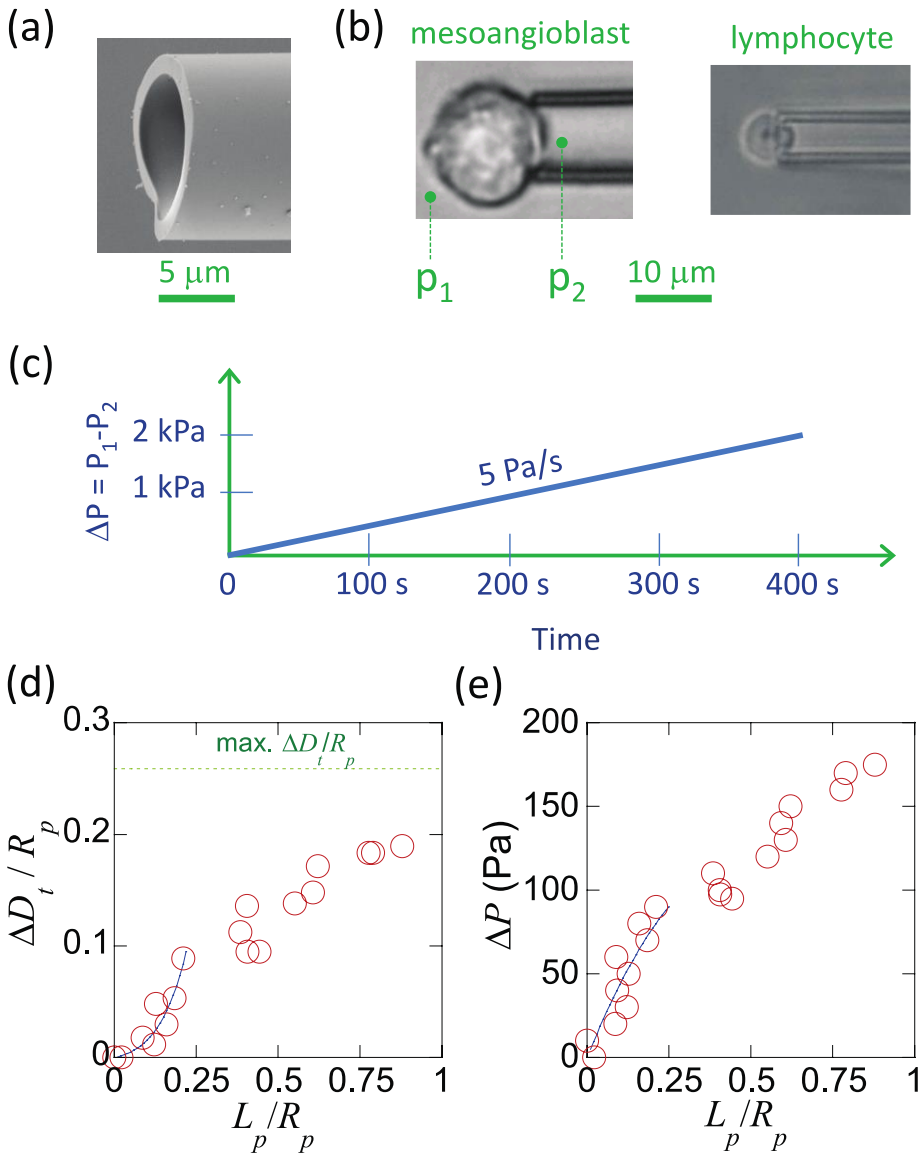

Figure 6. Micropipette aspiration experiments. (a) Electron microscope image of a glass microcapillary with an internal diameter $2R_p$ ~ 10 µm. (b) Optical images obtained during aspirations experiments of a resuspended mesoangioblast ($2R_p$ ~ 10 µm) and a lymphocyte ($2R_p$ ~ 5 µm). (c) Scheme of the ramp of differential pressure applied during the experiments with lymphocytes analyzed in this work. (d-e) Experimental results and curves obtained by fitting for an aspiration experiment with a lymphocyte; the equations 3 and 5 were fitted in the range $0 < L_p/R_p < 0.3$; in this example, R_c/R_p = 1.13, m_0 = 0.0610, ν = 0.434, En_1 = 485 Pa, n_1 = 0.386, E = 1.26 kPa.

DISCUSSION

For small deformations the cell behavior may be described as solid-like (25, 26), and the simplest approach is to describe the cell as a homogeneous, isotropic linear-elastic solid. Theret et al. obtained an analytical equation to compute the elastic modulus by modeling the cell as a homogeneous, isotropic non-compressible elastic half-space (35). Zhou et al. developed a numerical model for a spherical cell of non-compressible neo-Hookean material, fitting an equation that allows computing the elastic modulus of the cell (36). A linearized version for small deformation was obtained later (17). Li and Chen used a numerical model to develop an equation for a homogeneous, isotropic linear-elastic spherical cell (37). With their equation it was not possible to calculate the two parameters of the material, i.e. the elastic modulus and the Poisson's ratio. Besides, the structural nonlinearity of the problem, due to the contact between the cell and the surface of the microcapillary, was obviated in that interesting work.

In the previous models the only directly-measurable kinematic variable utilized in the equations is the distance advanced by the front of the cell, L_p (see figure 1). This election limits the possibilities of computing mechanical parameters.

The numerical study has made it possible to analyze the accuracy of the different models used to evaluate the elastic modulus of cells, studying the effect of the fillet radius and developing a method to assess both the Poisson's ratio and the elastic modulus. As illustrated in Figure 3, the equation analytically deduced by Theret et al. may result in a very significant error for E and this could be one of the reasons for the reported differences in the values of elastic modulus measured with different techniques (14). Besides, this study confirms also the adequateness of using the equation provided by Zhou et al. to estimate the elastic modulus when incompressibility ($\nu = 0.5$) is assumed. The equation by Zhou et al. or its linearized version (17) should be used instead of that given by Theret et al. in order to get a better accuracy. Our model will provide similar results to Zhou et al.'s equation in its range of validity and when $\nu = 0.5$ (as shown in Figure 3).

The equations introduced in the previous sections are useful to estimate the elastic parameters with the condition of testing cells with a size sufficiently close to the internal diameter of the micropipette, so that the transversal contraction ΔD_t is optically measurable. We tested this approach with lymphocytes, being an example of particularly small cells, and applied it only for the very small cells ($R_c \sim 1.1\ R_p$), due to the optical resolution limit. The measurements would be easier for larger cells, including resuspended adherent cells. With this technique, the elastic modulus measured in future experiments will be more accurate and a better agreement between the elastic parameters measured by different techniques is expected.

For gels, at short times, the Poisson's ratio is close to 0.5, given that the flow of internal water out of the gel is negligible and it behaves as an incompressible material. The Poisson ratio may be different for longer times, and values between 0.25 and 0.5 have been found for different gels (44, 45). In the case of cells, due to their small size, the characteristic diffusion time for water is very low, of the order of 10^{-2} s (46), and therefore cells can likely show a Poisson's ratio different from 0.5 in experiments taking

place from seconds to tens of seconds. The average Poisson's coefficient of 0.33 obtained for lymphocytes would indicate that the volume is not constant in the first stage of the aspiration process, though for larger deformations it could be reasonable to consider it nearly constant, as it is commonly assumed. The elastic modulus $E_{0.05}$ measured for the few experiments of low-size lymphocytes is not significantly different from the average modulus $E_{\nu=0.5}$ estimated for the whole set of experiments using the incompressible-material model by Zhou et al. (P = 0.44). These values are in the range of values measured previously for lymphocytes, by cell pocking or atomic force microscopy (290-1330 kPa) (21, 47, 48).

The results of the numerical model have also shown the importance of the fillet radius. We have reasoned that, for small fillet radius (as it is typically the case in micropipette aspiration), the roughness of the cell, due to the ruffles and microvilli, determines the effective value of the fillet radius to be considered in the analysis. Following this rational, we chose a practical value $R_f = R_p/20$. Henceforth, increasing the accuracy of the analysis, for instance for extremely rough or smooth cells, would require a careful analysis of the surface features of the cells and the fillet radius to produce a representative numerical model. An important consequence of the influence of the fillet radius is that for techniques where cells pass through constrictions or constriction arrays (24), where radii of curvature of contact surfaces are larger, it is critical to use constrictions with very similar curvatures to obtain reproducible results.

CONCLUSIONS

The method proposed in this article evaluates the Poisson's ratio and elastic modulus of cells from micropipette experiments where a large fraction of the volume of the cell stretches during times typically of the order from seconds to tens of seconds. Quantifying the Poisson's ratio by the proposed equations requires testing cells with a size close to the internal diameter of the microcapillary. The improved characterization of the elastic parameters of cells could be useful to establish mechanical differences between different cells types and to allow the comparison of the results obtained with different techniques. Besides, the method will be appropriate to be implemented in experiments with the micropipette aspiration technique and in future automated versions of this technique, allowing testing large numbers of cells in short times.

The study describes also the basis for future studies of the mechanical properties of lymphocytes, which will be of interest to evaluate the usefulness of the mechanical properties as a biomarker of T-cell state. The deformability of lymphocytes is a key property in relation to their migration ability, which is fundamental for infection recovery. Future automated systems to measure these properties could be valuable in the clinical practice.

This study has provided additionally an evaluation of the currently available models and equations to characterize the elastic modulus of cells (all of them assuming incompressible cells), quantifying their theoretical error as a function of the relative size of the cell.

Cite as: Esteban-Manzanares, G., González-Bermúdez, B., Cruces, J. et al. Improved Measurement of Elastic Properties of Cells by Micropipette Aspiration and Its Application to Lymphocytes. Ann Biomed Eng 45, 1375–1385 (2017). https://doi.org/10.1007/s10439-017-1795-7.

ACKNOWLEDGEMENTS

The authors would like to thank M. Carmen Álvarez for her help in preparing microscopy samples.

Tables

α_1	α_2	α_3	α_4	α_5
0.9259	-1.194	0.3711	15.96	0.1671

Table 1. Numerical values of the constants of equations (2) and (3), obtained for the range $1.1 < R_c/R_p < 1.5$.

β_1	β_2	β_3	β_4
0.561	-0.943	0.447	5.40

Table 2. Numerical values of the constants of equation (5) , obtained for the range $1.1 < R_c/R_p < 1.5$.

References

1. Di Carlo, D. 2012. A mechanical biomarker of cell state in medicine. J Lab Autom. 17, 32-42.

2. Gossett, D. R., H.T.K. Tse, S.A. Lee, Y. Ying, A.G. Lindgren, O.O. Yang, J. Rao, A.T. Clark and D. Di Carlo 2012. Hydrodynamic stretching of single cells for large population mechanical phenotyping. Proc. Natl. Acad. Sci. U. S. A. 109, 7630-7635.

3. Swift, J., I.L. Ivanovska, A. Buxboim, T. Harada, P.C.D.P. Dingal, J. Pinter, J.D. Pajerowski, K.R. Spinler, J. Shin, M. Tewari, F. Rehfeldt, D.W. Speicher and D.E. Discher 2013. Nuclear lamin-A scales with tissue stiffness and enhances matrix-directed differentiation. Science. 341, 1240104.

4. Boal, D. 2012. Mechanics of the cell. Cambridge University Press, Cambridge, United Kingdom.

5. Worthen, G. S., B. Schwab, E.L. Elson and G.P. Downey 1989. Mechanics of stimulated neutrophils - cell stiffening induces retention in capillaries. Science. 245, 183-186.

6. Nishino, M., H. Tanaka, H. Ogura, Y. Inoue, T. Koh, K. Fujita and H. Sugimoto 2005. Serial changes in leukcocyte deformability and whole blood rheology in patients with sepsis or trauma. Journal of Trauma-Injury Infection and Critical Care. 59, 1425-1431.

7. Poschl, J. M. B., P. Ruef and O. Linderkamp 2005. Deformability of passive and activated neutrophils in children with gram-negative septicemia. Scandinavian Journal of Clinical & Laboratory Investigation. 65, 333-339.

8. Suresh, S., J. Spatz, J.P. Mills, A. Micoulet, M. Dao, C.T. Lim, M. Beil and T. Seufferlein 2005. Connections between single-cell biomechanics and human disease states: Gastrointestinal cancer and malaria. Acta Biomaterialia. 1, 15-30.

9. Lois, C. and A. Alvarezbuylla 1994. Long-distance neuronal migration in the adult mammalian brain. Science. 264, 1145-1148.

10. Ip, J. E., Y. Wu, J. Huang, L. Zhang, R.E. Pratt and V.J. Dzau 2007. Mesenchymal stem cells use integrin beta 1 not CXC chemokine receptor 4 for myocardial migration and engraftment. Mol. Biol. Cell. 18, 2873-2882.

11. Bernal, A., L.M. Perez, B. De Lucas, N.S. Martin, A. Kadow-Romacker, G. Plaza, K. Raum and B.G. Galvez 2015. Low-intensity pulsed ultrasound improves the functional properties of cardiac mesoangioblasts. Stem Cell Reviews. 11, 852-865.

12. Engler, A. J., S. Sen, H.L. Sweeney and D.E. Discher 2006. Matrix elasticity directs stem cell lineage specification. Cell. 126, 677-689.

13. Wang, N., J.D. Tytell and D.E. Ingber 2009. Mechanotransduction at a distance: Mechanically coupling the extracellular matrix with the nucleus. Nature Reviews Molecular Cell Biology. 10, 75-82.

14. Rodriguez, M. L., P.J. McGarry and N.J. Sniadecki 2013. Review on cell mechanics: Experimental and modeling approaches. Appl. Mech. Rev. 65, 060801.

15. Bao, G. and S. Suresh 2003. Cell and molecular mechanics of biological materials. Nature Materials. 2, 715-725.

16. Hochmuth, R. M. 2000. Micropipette aspiration of living cells. J. Biomech. 33, 15-22.

17. Plaza, G. R., T.Q.P. Uyeda, Z. Mirzaei and C.A. Simmons 2015. Study of the influence of actin-binding proteins using linear analyses of cell deformability. Soft Matter. 11, 5435-5446.

18. Plaza, G. R., N. Marí, B.G. Gálvez, A. Bernal, G.V. Guinea, R. Daza, J. Pérez-Rigueiro, C. Solanas and M. Elices 2014. Simple measurement of the apparent viscosity of a cell from only one picture: Application to cardiac stem cells. Physical Review E. 90, 052715.

19. Yeung, A. and E. Evans 1989. Cortical shell-liquid core model for passive flow of liquid-like spherical cells into micropipets. Biophys. J. 56, 139-149.

20. Haase, K. and A.E. Pelling 2015. Investigating cell mechanics with atomic force microscopy. Journal of the Royal Society Interface. 12, 20140970.

21. Daza, R., J. Cruces, M. Arroyo-Hernandez, N. Mari-Buye, M. De la Fuente, G.R. Plaza, M. Elices, J. Perez-Rigueiro and G.V. Guinea 2015. Topographical and mechanical characterization of living eukaryotic cells on opaque substrates: Development of a general procedure and its application to the study of non-adherent lymphocytes. Physical Biology. 12, 026005-026005.

22. Butler, J. P. and S.M. Kelly 1998. A model for cytoplasmic rheology consistent with magnetic twisting cytometry. Biorheology. 35, 193-209.

23. Guck, J., S. Schinkinger, B. Lincoln, F. Wottawah, S. Ebert, M. Romeyke, D. Lenz, H.M. Erickson, R. Ananthakrishnan, D. Mitchell, J. Kas, S. Ulvick and C. Bilby 2005. Optical deformability as an inherent cell marker for testing malignant transformation and metastatic competence. Biophys. J. 88, 3689-3698.

24. Lange, J. R., J. Steinwachs, T. Kolb, L.A. Lautscham, I. Harder, G. Whyte and B. Fabry 2015. Microconstriction arrays for high-throughput quantitative measurements of cell mechanical properties. Biophysical Journal. 109, 26-34.

25. Trepat, X., L. Deng, S.S. An, D. Navajas, D.J. Tschumperlin, W.T. Gerthoffer, J.P. Butler and J.J. Fredberg 2007. Universal physical responses to stretch in the living cell. Nature. 447, 592-+.

26. Zhou, E. H., F.D. Martinez and J.J. Fredberg 2013. CELL RHEOLOGY mush rather than machine. Nature Materials. 12, 184-185.

27. Luo, T., K. Mohan, P.A. Iglesias and D.N. Robinson 2013. Molecular mechanisms of cellular mechanosensing. Nature Materials. 12, 1064-71.

28. Stewart, M. P., J. Helenius, Y. Toyoda, S.P. Ramanathan, D.J. Muller and A.A. Hyman 2011. Hydrostatic pressure and the actomyosin cortex drive mitotic cell rounding. Nature. 469, 226-230.

29. Plaza, G. R. and T.Q.P. Uyeda 2013. Contraction speed of the actomyosin cytoskeleton in the absence of the cell membrane. Soft Matter. 9, 4390-4400.

30. EVANS, E. 1973. New membrane concept applied to analysis of fluid shear-deformed and micropipet-deformed red blood-cells. Biophys. J. 13, 941-954.

31. EVANS, E. and A. YEUNG 1989. Apparent viscosity and cortical tension of blood granulocytes determined by micropipet aspiration. Biophys. J. 56, 151-160.

32. Needham, D. and R.M. Hochmuth 1990. Rapid flow of passive neutrophils into a 4 mu-M pipette and measurement of cytoplasmic viscosity. Journal of Biomechanical Engineering-Transactions of the Asme. 112, 269-276.

33. Discher, D. E., D.H. Boal and S.K. Boey 1998. Simulations of the erythrocyte cytoskeleton at large deformation. II. micropipette aspiration. Biophys. J. 75, 1584-1597.

34. Svetina, S., G. Kokot, T.S. Kebe, B. Zeks and R.E. Waugh 2016. A novel strain energy relationship for red blood cell membrane skeleton based on spectrin stiffness and its application to micropipette deformation. Biomechanics and Modeling in Mechanobiology. 15, 745-758.

35. Theret, D. P., M.J. Levesque, M. Sato, R.M. Nerem and L.T. Wheeler 1988. The application of a homogeneous half-space model in the analysis of endothelial-cell micropipette measurements. Journal of Biomechanical Engineering-Transactions of the Asme. 110, 190-199.

36. Zhou, E. H., C.T. Lim and S.T. Quek 2005. Finite element simulation of the micropipette aspiration of a living cell undergoing large viscoelastic deformation. Mechanics of Advanced Materials and Structures. 12, 501-512.

37. Li YongSheng and Chen WeiYi 2013. Finite element analysis of micropipette aspiration considering finite size and compressibility of cells. Science China-Physics Mechanics & Astronomy. 56, 2208-2215.

38. Janeway, C., P. Travers, M. Walport and M. Shlomchik 2001. Immunobiology: The immune system in health and disease.

39. Alonso-Fernandez, P. and M. De la Fuente 2011. Role of the immune system in aging and longevity. Current Aging Science. 4, 78-100.

40. Trickey, W. R., G.M. Lee and F. Guilak 2000. Viscoelastic properties of chondrocytes from normal and osteoarthritic human cartilage. Journal of Orthopaedic Research. 18, 891-898.

41. Alexandrov, V. M.andD. A. Pozharskii 2001. Three-dimensional contact problems. Kluwer Academic Publishers - Springer Netherlands,.

42. Majstoravich, S., J.Y. Zhang, S. Nicholson-Dykstra, S. Linder, W. Friedrich, K.A. Siminovitch and H.N. Higgs 2004. Lymphocyte microvilli are dynamic, actin-dependent structures that do not require wiskott-aldrich syndrome protein (WASp) for their morphology. Blood. 104, 1396-1403.

43. Friedmann, A., A. Hoess, A. Cismak and A. Heilmann 2011. Investigation of cell-substrate interactions by focused ion beam preparation and scanning electron microscopy. Acta Biomaterialia. 7, 2499-2507.

44. Geissler, E. and A.M. Hecht 1981. The poisson ration in polymer gels .2. Macromolecules. 14, 185-188.

45. Urayama, K., T. Takigawa and T. Masuda 1993. Poisson ratio of poly(vinyl alcohol) gels. Macromolecules. 26, 3092-3096.

46. Phillips, R.,J. Kondev,J. Theriot and H. Garcia 2012. Physical Biology of the Cell. Garland Science, New York.

47. Zahalak, G. I., W.B. Mcconnaughey and E.L. Elson 1990. Determination of cellular mechanical-properties by cell poking, with an application to leukocytes. Journal of Biomechanical Engineering-Transactions of the Asme. 112, 283-294.

48. Cai, X., X. Xing, J. Cai, Q. Chen, S. Wu and F. Huang 2010. Connection between biomechanics and cytoskeleton structure of lymphocyte and jurkat cells: An AFM study. Micron. 41, 257-262.